

Titanium leaching from red mud by diluted sulfuric acid at atmospheric pressure

S. Agatzini-Leonardou, P. Oustadakis, P.E. Tsakiridis*, Ch. Markopoulos

Department of Mining and Metallurgical Engineering, Laboratory of Metallurgy, National Technical University of Athens, 9 Iroon Polytechniou Street, 157 80 Zografou, Athens, Greece

Received 14 September 2007; received in revised form 26 November 2007; accepted 10 January 2008
Available online 20 January 2008

Abstract

Laboratory-scale research has focused on the recovery of titanium from red mud, which is obtained from bauxite during the Bayer process for alumina production. The leaching process is based on the extraction of this element with diluted sulfuric acid from red mud under atmospheric conditions and without using any preliminary treatment. Statistical design and analysis of experiments were used, in order to determine the main effects and interactions of the leaching process factors, which were: acid normality, temperature and solid to liquid ratio. The titanium recovery efficiency on the basis of red mud weight reached 64.5%. The characterization of the initial red mud, as well as this of the leached residues was carried out by X-ray diffraction, TG-DTA and scanning electron microscopy.

© 2008 Elsevier B.V. All rights reserved.

Keywords: Red mud; Titanium; Leaching; Sulfuric acid

1. Introduction

Bauxite contains high percentage of aluminum hydroxides and is therefore largely used for the production of alumina (Al_2O_3) through the Bayer chemical process, which is based on the reaction with sodium hydroxide under heat and pressure. The overall refining of bauxite to alumina through the Bayer process implies the production of a large quantity of a solid waste called “red mud” [1].

Red mud generally exits the process stream as a highly alkaline slurry (pH 10–12.5) with 15–30% solids and it is pumped away for appropriate disposal [2,3]. It is a complex material whose chemical and mineralogical composition varies widely, depending upon the source of bauxite and the technological process parameters. It contains six major constituents, namely, Fe_2O_3 , Al_2O_3 , SiO_2 , TiO_2 , Na_2O and CaO and small quantities of numerous minor/trace elements (as oxides) such as V, Ga, Cr, P, Mn, Cu, Cd, Ni, Zn, Pb, Mg, Zr, Hf, Nb, U, Th, K, Ba, Sr, rare earths, etc. Every red mud is composed of as many as 14–21 mineral phases [4–6]. Its brick red color is due to the iron oxides.

At all the world's 85 alumina plants, 1.0–1.6 tons of red mud is generated per ton of alumina and it is estimated that over 66 million tons of this waste are impounded annually in the world. The disposal of such a large quantity of this alkaline waste sludge is expensive (up to 1–2% of the alumina price), as it requires a large disposal area (approximately 1 km^2 per 5 years for a 1 Mtpy alumina plant) and causes a number of environmental problems [2]. The neutralization of red mud and its adequate treatment to allow its reuse seem to be the realistically convenient steps for the disposal of this industrial residue [1]. In Greece, the annual production of bauxitic red mud, from the alumina processing plant, is approximately 500,000 tons/year. The red mud slurry has a concentration of 500 g/l and bulk density of 1.3 g/l [7,8].

Today, disposal and utilization of red mud are problems for all alumina industries in the world. Red mud has been used in absorbents, building materials, catalysts, fillers and pigments [9–11]. It is very fine, difficult to settle and filter and is highly alkaline. However, it also contains a range of valuable constituents, such as titanium, and it may be considered secondary raw material for their recovery. Titanium metal is extraordinarily strong and exceptionally lightweight – as strong as steel with only 60% of its weight – and is bio-inert and resistant to corrosion. However, expensive and complex processing costs are only

* Corresponding author. Tel.: +30 210 7722234; fax: +30 210 7722218.
E-mail address: ptsakiri@central.ntua.gr (P.E. Tsakiridis).

tolerated by the aerospace and biochemical industries, where the advantages of using titanium outweigh the expense.

An analysis of the relative literature indicates that there is no simple method for recovery of titanium from red mud. There are two possible processes to manage red mud residue for titanium recovery: pyrometallurgical and hydrometallurgical. Pyrometallurgical smelting flowsheets usually includes extracting pig iron, a soda and alumina-rich stream (which can be recycled back to the Bayer process) and a slag containing titanium, silica, lime, residual alumina and magnesium. The slag phase is then further treated to produce a high-grade titania product, plus a residue which could be used as feed to a cement kiln.

Iron, titanium and aluminum values can be recovered from red mud residue by calcining it, preferably between 800 °C and 1350 °C, and smelting the material with a carbonaceous reducing agent in an electric furnace, thus obtaining molten iron, and a slag containing substantially all the titania, alumina and silica [12]. The metallic iron can be, then, separated and the slag is digested with aqueous sulfuric acid, preferably of at least 60% concentration. A solution of aluminum and titanium sulfates, and an insoluble residue of silica is obtained. Uzhidy et al. suggested selective chlorination of iron from red mud. The red mud was calcined in reducing atmosphere at 800–900 °C and chlorinated at 500 °C to obtain chloride of alumina [13]. Ercag and Apak mixed the red mud with dolomite and coke, pelletized and sintered the mixture at 1100 °C, and finally smelted it at 1550 °C to produce pig iron and a slag containing titanium [14]. The slag was then leached with 30% H₂SO₄ at 90 °C. The titanium recovery efficiency on the basis of slag weight was 84.7%. Kasliwal and Sai proposed a process for the enrichment of titanium dioxide in red mud [15]. The procedure employed is leaching the red mud with hydrochloric acid followed by roasting the leached residue with sodium carbonate. Leaching kinetics data, regarding various red mud constituents were experimentally obtained using a stirred batch reactor. In this process TiO₂ recovery increased from 18% to 36% in the first step and further to 76% after the second step.

While pyrometallurgical processes face problems such as high energy consumption and generation of worthless residues, hydrometallurgical processes are still a promise for the future, despite the research done in this field. Hydrometallurgical processes could offer an interesting alternative for titanium recycling, if iron dissolution is controlled.

Bhatnagar et al. proposed a process for the recovery of titanium dioxide from red mud, by sulfuric acid leaching, followed by hydrolysis and calcinations [16]. The final TiO₂ recovery reached at 70%. Zimmer et al. suggested a red mud digestion process, with concentrated sulfuric acid, in order to produce sulfates that can be leached out with water [17]. The final solution can be then heated at a pH value of 1 to precipitate titanium oxide hydrate by hydrolysis. Damodaran and Gupta examined the recovery of alumina from red mud, by hydrochloric acid (5N) leaching, followed by sulfuric acid digestion [18]. Sayan and Bayramoglu examined the recovery of titanium from red mud, with sulfuric acid leaching by statistically designed experiments [19]. They reported that around 70% of Ti recovery was reached by leaching with 4N sulfuric acid, at 90 °C.

The aim of the present research work was to investigate the possibility of titanium recovery from red mud, with sulfuric acid leaching. Factorial design of experiments and statistical analysis of the obtained data were used to determine the main effects and interactions of the chosen factors and select the optimum conditions. The factors studied were: sulfuric acid concentration, temperature and solid to liquid ratio. The initial and the resulting leached residues were investigated by, X-ray diffraction, TG-DTA and scanning electron microscopy.

2. Experimental

Uncausticised red mud from aluminum of Greece Company was used as received. The red mud leaching procedure was carried out under atmospheric pressure. All batch experiments were conducted in a 500-ml five-necked, round bottomed split reactor, which was fitted with a glass stirrer, a vapor condenser and a thermometer. In all the experiments, a constant stirring speed was used to ensure suspension of the particles. Heating was provided by an electrical mantle and the temperature of the liquid was controlled by a Fisons Scientific Apparatus monitor. A typical run was carried out as follows: specified amounts of preheated sulfuric acid of known concentration and red mud were loaded into the glass reactor. The stirring speed was maintained constant by means of a digital controlled stirrer. At the end of the runs, the content of the reactor was filtered under vacuum. The resulting leached residues were washed with water by re-pulping, dried overnight at 110 °C and weighed.

The initial red mud, as well as the leached residues and leach liquors were analyzed chemically, using a PerkinElmer Model 4100 atomic absorption spectrometer. The mineralogical analysis was carried out by X-ray diffraction (XRD), using a Siemens D5000 diffractometer with nickel-filtered CuK α radiation (=1.5405 Å), 40 kV and 30 mA. TG/DTA analysis was conducted with a Setaram-Labsys thermal analyzer. Type S-thermocouple is used for temperature measurements in this instrument. The sample was placed in a ceramic crucible and heated from room temperature to 1000 °C at a heating rate of 5 °C/min using air as a medium under static condition. TG/DTA were done simultaneously. The morphology of the leached residues was also examined by scanning electron microscopy (SEM) using a Jeol 6380LV scanning electron microscope. Experimental conditions involved 15 kV accelerating voltage. Chemical composition of the samples was carried out by an Oxford INCA electron dispersive spectrometer (EDS) connected to the SEM. Finally, the particle size distribution of the initial red mud was determined by a Cilas-Model 1064 laser scattering particle size distribution analyzer. An amount of 0.1 g of sample powder was put in 100 ml of ethanol and underwent dispersion treatment by an ultrasonic dispersion unit for 60 s.

3. Results and discussions

3.1. Chemical and mineralogical characteristics of red mud used

Iron, aluminum and titanium oxide are the major constituents of the red mud used, which has the following composition (%)

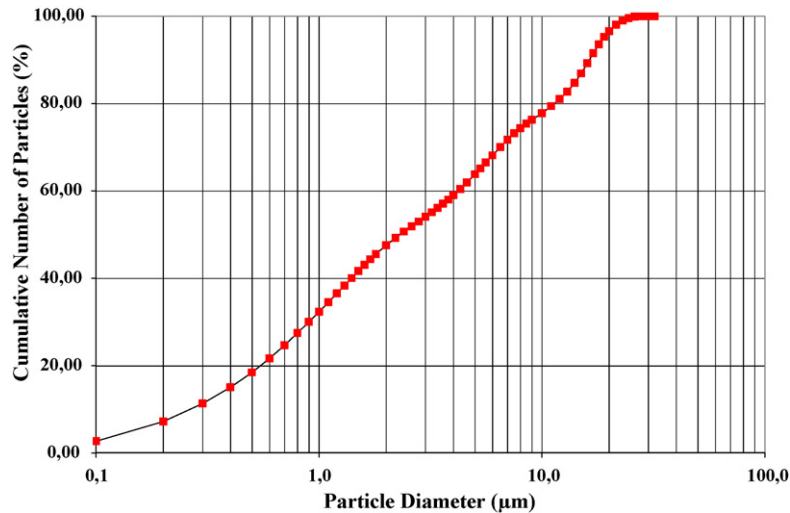


Fig. 1. Particle size distributions of the red mud used by a laser scattering analyzer.

by wt.): Fe_2O_3 , 41.30; Al_2O_3 , 21.20; TiO_2 , 7.10; SiO_2 , 5.35; CaO , 11.02; MgO , 0.25; K_2O , 0.15; Na_2O , 2.15; Cr_2O_3 , 0.31; SO_3 , 0.65; loss on ignition, 10.50. Its particle size distribution is given in Fig. 1. It was found that 50% of the red mud was below $2.4 \mu\text{m}$, whereas 100% of the material was below $28 \mu\text{m}$. The mean diameter of the precipitate was computed at $5.5 \mu\text{m}$.

According to the XRD data (Fig. 2), the red mud contains mainly hematite [Fe_2O_3], diaspore [$\text{AlO}(\text{OH})$], gibbsite [$\text{Al}(\text{OH})_3$], calcite [CaCO_3], devitrite [$\text{Na}_2\text{Ca}_3\text{Si}_6\text{O}_{16}$] and katoite [$\text{Ca}_3\text{Al}_2\text{SiO}_4(\text{OH})_8$]. Quartz [SiO_2], anatase [TiO_2], kaolinite [$\text{Al}_2\text{Si}_2\text{O}_5(\text{OH})_4$] and goethite [FeOOH] are also present as minor constituents.

The results of the differential thermal analysis (DTA) and thermal analysis (TG) of the initial red mud sample are given in Fig. 3. The TG diagram shows four steps for the weight loss. The first one occurred in the range of $30\text{--}145^\circ\text{C}$ (weight loss was about 1% of the total weight), corresponding to the evaporation of physically adsorbed water. The second and the third one occurred in the range of $145\text{--}440^\circ\text{C}$ (weight loss: 4%) and in the range of $440\text{--}600^\circ\text{C}$ (weight loss: 3.15%) correspondingly, and they were attributed to the loss of chemically adsorbed water (mainly due to the decomposition of gibbsite and diaspore). Finally, the fourth one occurred in the range of $600\text{--}800^\circ\text{C}$ (weight loss was about 3.69% of the total weight), which cor-

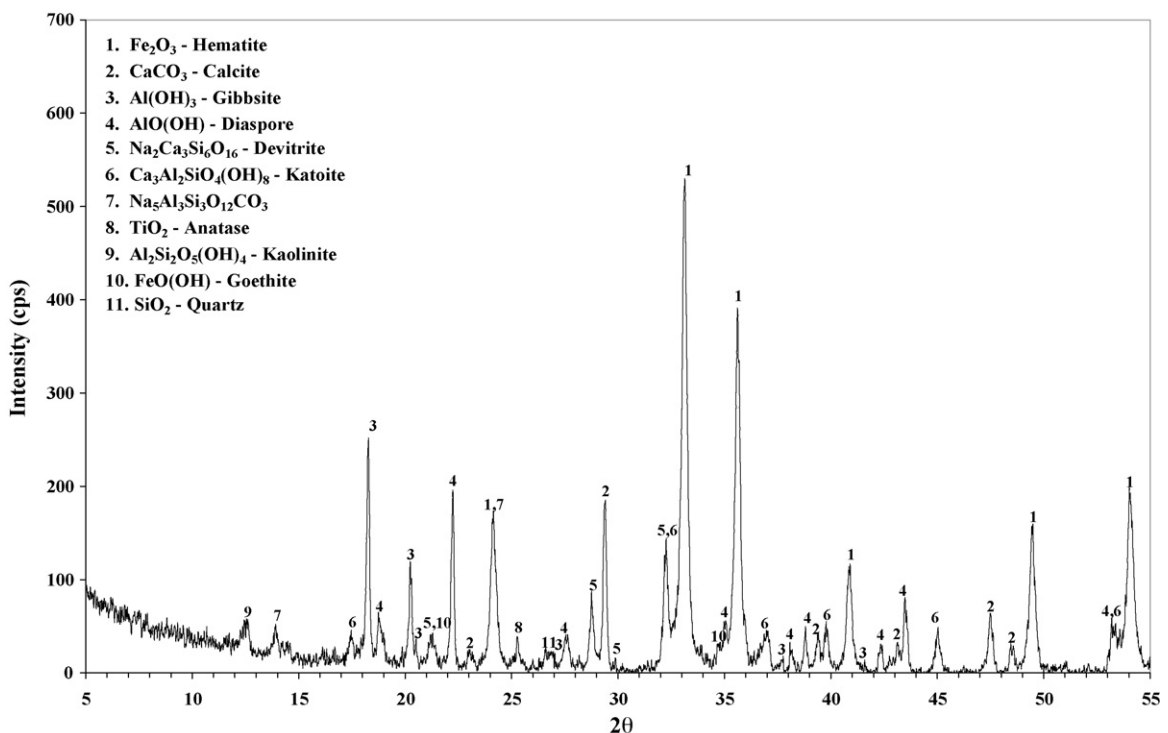


Fig. 2. Mineralogical phases of red mud used.

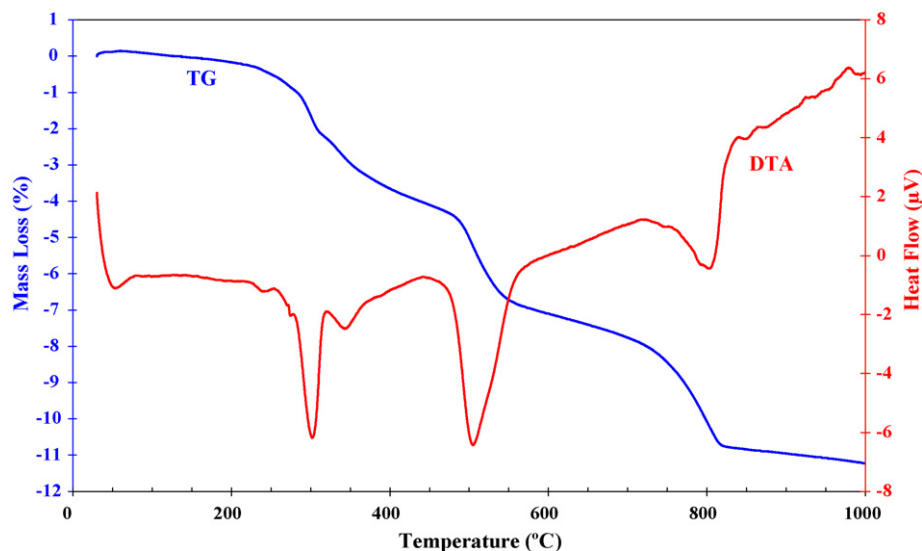
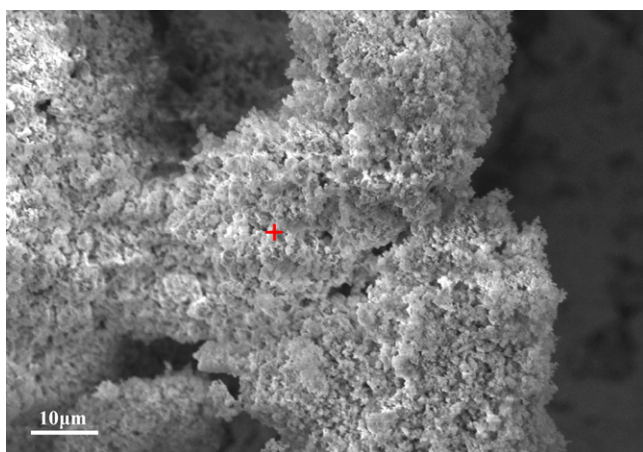


Fig. 3. TG/DTA curves of the initial red mud sample.

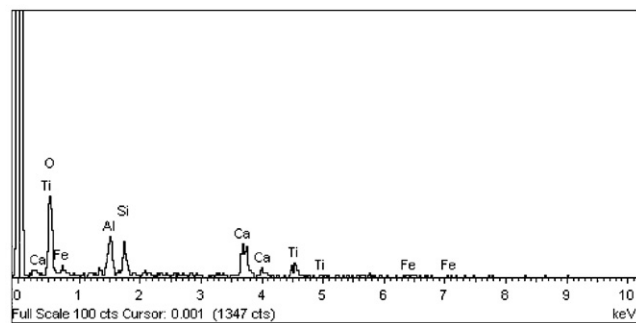
responds to the release of CO_2 during calcinations of calcite. The endothermic peak between 270°C and 320°C , on the DTA curve, is associated with the dehydration of gibbsite to form α -alumina. The second endothermic peak at 510°C was attributed to the decomposition of diasporite [20]. The endothermic peak at about 805°C resulted from the decomposition of calcite. Finally,

the low mass loss, without revealing a peak, occurring after 805°C can be related to sodium aluminum carbonate silicate decomposition in the red mud.

SEM micrographs show that the particles of red mud used was in poorly crystallized forms. Hematite presents globular structure and was detected in the form of aggregates of fine crystallites (Fig. 4). The aggregates had an irregular shape and a homogeneous size of about $5\ \mu\text{m}$ (longest dimension). Gibbsite was detected in the form of large hexagonal plate-like crystals with size from $5\ \mu\text{m}$ to $20\ \mu\text{m}$ (Fig. 5). EDS studies revealed the presence of Fe and Al, whereas smaller amounts of Si, Ca and Ti were also found. Iron and titanium corresponded to small granules, homogeneously distributed, while the larger flat particles present, mainly consisted of Al.



(a) Aggregates of fine crystallites



(b) Composition of the above marked spot

Fig. 4. SEM micrographs of the initial red mud sample.

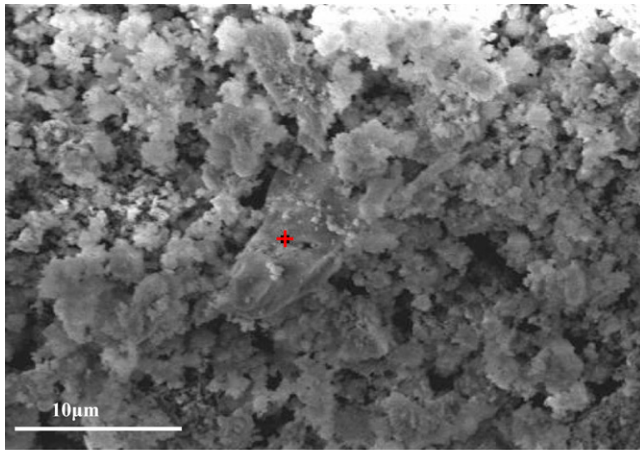
3.2. Statistical study of the red mud leaching process

Factorial design and analysis of experiments were used in order to determine the main effects and interactions of the leaching factors [21]. The factors studied and their levels, for red mud leaching by diluted sulfuric acid, are shown in Table 1. Parameters, which were kept constant during experimentation, were:

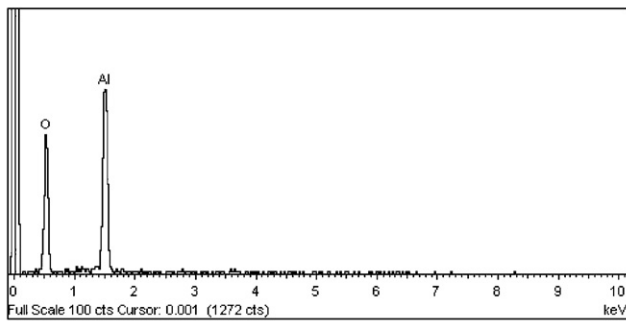
- Stirring speed = 700 r.p.m.
- Reaction time = 4 h.

Table 1
Red mud leaching by diluted sulfuric acid—minimum and maximum levels of variables

Factor	Variables	Low level (–)	High level (+)	Units measured
A	Acid normality	3	6	N
B	Temperature	40	60	$^\circ\text{C}$
C	Solid to liquid ratio	5	20	%



(a) Large hexagonal plate-like crystals of gibbsite



(b) Composition of the above marked spot

Fig. 5. SEM micrographs of the initial red mud sample.

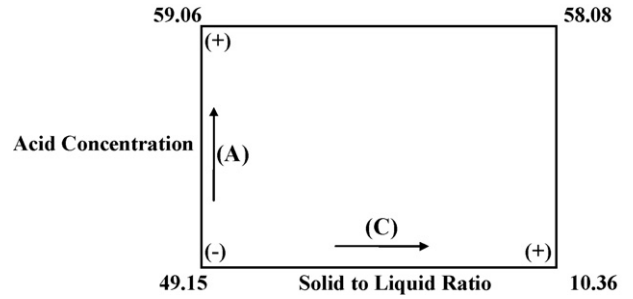


Fig. 6. Two-way table showing the interaction between acid concentration and solid to liquid ratio (AC).

The main response under investigation was the percentage of titanium recovery in the leach liquor. The leaching percentages of iron and aluminum are given in Table 2. As can be seen in Table 2, titanium leaching varied from 9.30% to 64.53%. Under the present experimental conditions iron dissolution varied from 4.66% to 46.01%, whereas aluminum leaching reached 37%. The red mud leaching present an increase in dissolution of Ti depending, mainly, upon the concentration of acid and solid to liquid ratio. It was observed that when a solid to liquid ratio of 5% is used, titanium leaching was increased, especially at higher acid concentration. On the other hand, iron and aluminum present lower leaching values at higher temperature and higher solid to liquid ratio level.

To study the main effects and interactions of the factors on the titanium leaching, a Yates’ analysis and an analysis of variance were carried out on the percentage of Ti recovery from red

Table 2
% recovery of metals in the leach liquor after leaching by diluted sulfuric acid

Treatment Code	Variables studied			Titanium (%)	Iron (%)	Aluminum (%)
	A	B	C			
1	–	–	–	47.51 ± 1.37	25.06 ± 2.73	45.93 ± 1.29
a	+	–	–	53.60 ± 1.37	40.45 ± 2.73	36.22 ± 1.29
b	–	+	–	50.80 ± 1.37	24.50 ± 2.73	40.42 ± 1.29
ab	+	+	–	64.53 ± 1.37	46.01 ± 2.73	37.09 ± 1.29
c	–	–	+	9.30 ± 1.37	4.66 ± 2.73	35.22 ± 1.29
ac	+	–	+	53.30 ± 1.37	23.94 ± 2.73	40.95 ± 1.29
bc	–	+	+	11.43 ± 1.37	6.79 ± 2.73	39.26 ± 1.29
abc	+	+	+	62.85 ± 1.37	37.57 ± 2.73	34.66 ± 1.29

Table 3
Yates’ analysis and analysis of variance—response: % Ti leaching by diluted sulfuric acid

Treatment code	Response Ti leaching (%)	Yates’ analysis					Analysis of variance			
		1	2	3	Divisor	Effects	Identification	$t = \text{eff}/S_e$	$t_{0.01} \Phi = 8$	Significance at $\alpha = 0.01$
(1)	47.51 ± 1.37	101.10	216.43	353.30	8	44.16 ± 0.485	Average			
a	53.60 ± 1.37	115.33	136.88	115.25	4	28.81 ± 0.97	A	29.70	3.36	S
b	50.80 ± 1.37	62.60	19.83	25.90	4	6.48 ± 0.97	B	6.68	3.36	S
ab	64.53 ± 1.37	74.28	95.42	15.07	4	3.77 ± 0.97	AB	3.88	3.36	S
c	9.30 ± 1.37	6.09	14.23	–79.55	4	–19.89 ± 0.97	C	–20.50	3.36	S
ac	53.30 ± 1.37	13.74	11.68	75.60	4	18.90 ± 0.97	AC	19.48	3.36	S
bc	11.43 ± 1.37	44.00	7.65	–2.55	4	–0.64 ± 0.97	BC	–0.66	3.36	NS
abc	62.85 ± 1.37	51.42	7.42	–0.22	4	–0.06 ± 0.97	ABC	–0.06	3.36	NS

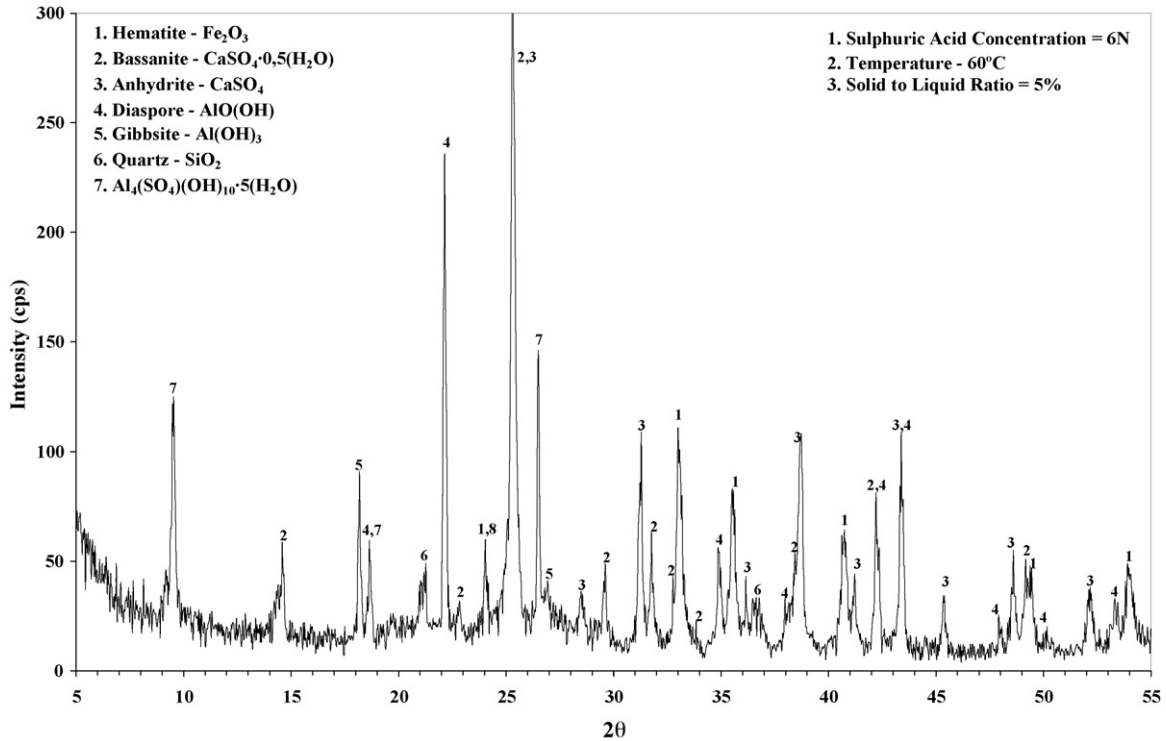


Fig. 7. X-ray diffraction of the red mud leached residue.

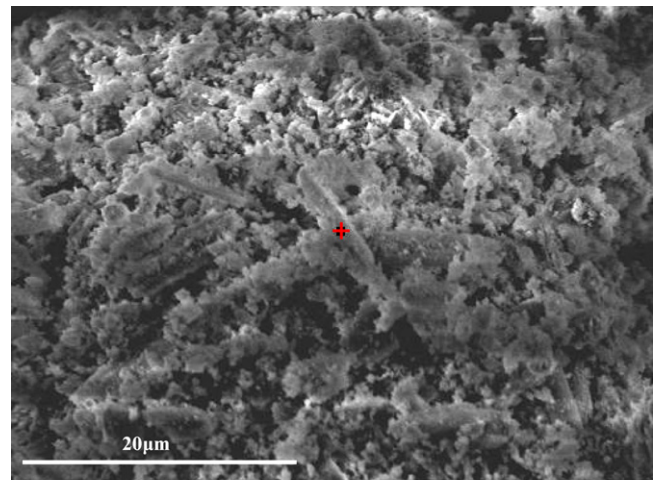
mud by diluted sulfuric acid leaching. The results are shown in Table 3.

The main effects A (acid normality) and B (temperature) and the two-factor interactions AB and AC were found to be statistically significant at $\alpha = 0.01$ and positives. On the other hand the main effect of solid to liquid ratio (C) was also found to be statistically significant at $\alpha = 0.01$, but negative. In the range of variables studied, the acid normality (A) had the largest effects with a wide gap separating it from the remaining contrasts. The interaction AB seemed plausible as well, being non-additive of a pair of influential factors.

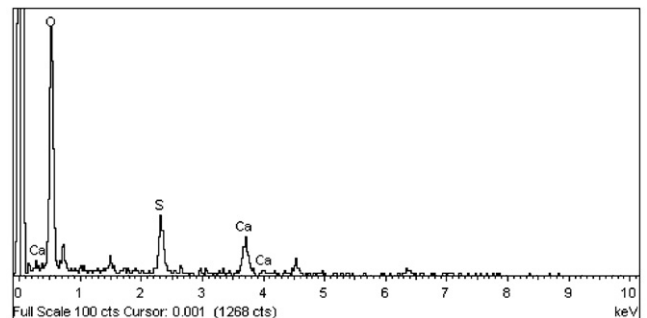
It should be stressed, however, that because of statistically significant interaction AC, the main effects should not be individually interpreted but the interacting variables should be considered jointly [21]. Thus, as Fig. 6 shows, the acid concentration (A) interacted with the solid to liquid ratio (C). The interaction occurs because at the high level of acid concentration the decrease of solid to liquid ratio causes higher titanium leaching.

The existence of statistically significant interactions indicated that a model, based on the main effects only, would not be suitable and that the response surface was curved in the particular region of the present design. Based on the above, the suggested “best” fitting model for titanium recovery, in the ranges of variables studied and under the present conditions of experimentation, is the following:

$$Y = 44.16 + 14.41X_1 + 3.24X_2 - 9.94X_3 + 1.88X_1X_2 + 9.45X_1X_3 \quad (1)$$

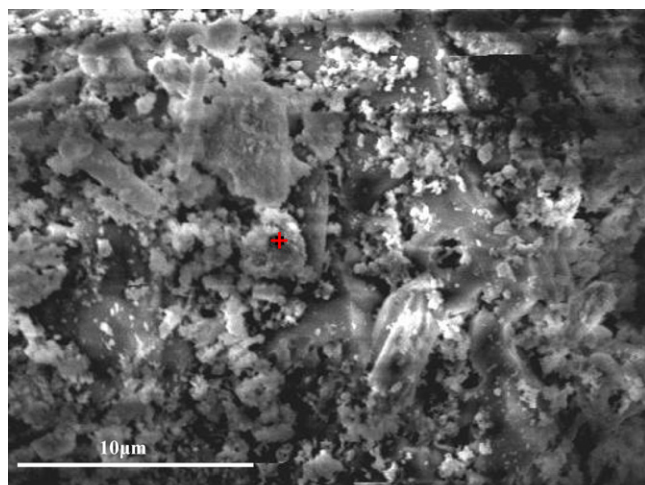


(a) Calcium sulfate needle-like crystals

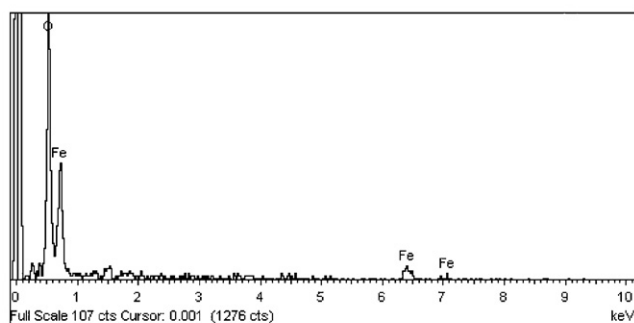


(b) Composition of the above marked spot

Fig. 8. SEM micrographs of red mud leached residue.



(a) Spheroid grains of hematite



(b) Composition of the above marked spot

Fig. 9. SEM micrographs of red mud leached residue.

where Y is the predicted value of titanium recovery from red mud and X_1 , X_2 and X_3 are coded variables, related to the natural variables by the following equations:

- $\bar{d}_1 = (\text{acid normality} - 4.5)/1.5$;
- $\bar{d}_2 = (\text{temperature} - 50)/10$;
- $\bar{d}_3 = (\text{solid to liquid ratio} - 12.5)/7.5$.

Based on the statistical analysis of the results, the optimum conditions determined for titanium leaching, from red mud by diluted sulfuric acid, were: acid normality = 6N, temperature = 60 °C and solid to liquid ratio = 5%.

3.3. Characterization of the leached residues

The X-ray diffraction data of the residue, after leaching by diluted sulfuric acid, at the optimum leaching conditions is presented in Fig. 7. Its main mineralogical phases were anhydrite (CaSO_4) and bassanite ($\text{CaSO}_4 \cdot 0.5\text{H}_2\text{O}$). The dissolution of Ca^{2+} red mud content into the system, led to the production of the above secondary precipitates. The main peaks were sharper and with higher intensity a fact that was attributed to the grain size and the degree of crystallinity of the two main products. Although the titanium phases is more or less leached within 4 h of leaching with 6N H_2SO_4 at 60 °C, the dissolution of diaspor

was found to be relative insignificant even after 4 h of leaching. Devitrite ($\text{Na}_2\text{Ca}_3\text{Si}_6\text{O}_{16}$) and $\text{Na}_5\text{Al}_3\text{Si}_3\text{O}_{12}\text{CO}_3$ seem to have been fully leached. The $\text{Al}_4(\text{SO}_4)(\text{OH})_{10} \cdot 5(\text{H}_2\text{O})$ phase observed in the leach residue has possibly formed from the re-crystallization of the dissolved Al^{3+} , mainly from the aluminum hydroxide phases, in the presence of the sulfates anions excess.

The results of the mineralogical analysis by X-ray diffraction were also confirmed by electron microscopic observations. As shown in Fig. 8, anhydrite and bassanite consisted of needle-like crystals of 5–20 μm in length and 1–5 μm in diameter. As the leaching reaction proceeded, iron decreased slightly, while aluminum, titanium, silicon and sodium decreased more markedly. The elements that hold or increased their composition were sulfur, calcium because of the formation of CaSO_4 , $\text{CaSO}_4 \cdot 0.5\text{H}_2\text{O}$ and $\text{Al}_4(\text{SO}_4)(\text{OH})_{10} \cdot 5(\text{H}_2\text{O})$ phases, in the leach residue. Hematite, which was detected in the form of aggregates of fine crystallites, presented spheroid particle/grains (Fig. 9).

4. Conclusions

The results obtained in the present work showed that titanium can be leached from the solid waste called red mud, which is obtained from bauxite during the Bayer process for alumina production, by diluted sulfuric acid.

The “Aluminum of Greece” red mud characterization showed that it was a very fine-grained powder, with a mean diameter of about 5.5 μm . It contained mainly hematite, diaspor, gibbsite and calcite, whereas TiO_2 content was about 7%. Three endothermic peaks were determined on the DTA curve and 10.8% of the total mass loss was observed on the TG, in the range of 25–1000 °C. SEM observations reveal that the red mud used was poorly crystallized. Hematite presented globular structure and was detected with the form of aggregates of fine crystallites, whereas gibbsite consisted of large hexagonal plate-like crystals.

A statistically designed experiment was performed to investigate the recovery of titanium content of the red mud, with diluted sulfuric acid leaching. The titanium recovery efficiency, on the basis of red mud weight, reached 64.5% at the following the optimum conditions: acid normality = 6N, temperature = 60 °C and solid to liquid ratio = 5%. At those conditions, iron leaching reached 46%, whereas that of aluminum did not exceed 37%.

The main mineralogical phases of the leached residues were anhydrite (CaSO_4) and bassanite ($\text{CaSO}_4 \cdot 0.5\text{H}_2\text{O}$). The detection of $\text{Al}_4(\text{SO}_4)(\text{OH})_{10} \cdot 5(\text{H}_2\text{O})$ phase was attributed to the re-crystallization of the dissolved Al^{3+} , in the presence of the sulfates anions excess. After 4 h of leaching, the dissolution of diaspor was found to be relative insignificant.

References

- [1] C. Brunori, C. Cremisini, P. Massanisso, V. Pinto, L. Torricelli, Reuse of a treated red mud bauxite waste: studies on environmental compatibility, *J. Hazard. Mater.* 117 (1) (2005) 55–63.
- [2] A.R. Hind, S.K. Bhargava, S.C. Grocott, The surface chemistry of Bayer process solids: a review, *Colloids Surf. A: Physicochem. Eng. Aspects* 146 (1–3) (1999) 359–374.

- [3] I. Paspaliaris, A. Karalis, The effect of various additives on diasporic bauxite leaching by the Bayer process, *Light Met.* (1993) 35–39.
- [4] Yong Liu, LinF Chuxia, Yonggui Wu, Characterization of red mud derived from a combined Bayer process and bauxite calcination method, *J. Hazard. Mater.* 146 (1–2) (2007) 255–261.
- [5] K. Solymar, I. Sajo, J. Steiner, J. Zoldi, Characteristics and separability of red mud, *Light Met.* (1992) 209–223.
- [6] L. Santona, P. Castaldi, P. Melis, Evaluation of the interaction mechanisms between red muds and heavy metals, *J. Hazard. Mater.* 136 (2) (2006) 324–329.
- [7] S.E. Poulos, M.B. Collins, C. Pattiaratchi, A. Cramp, W. Gull, M. Tsimplis, G. Papatheodorou, Oceanography and sedimentation in the semi-enclosed, deep-water Gulf of Corinth (Greece), *Marine Geol.* 134 (3–4) (1996) 213–235.
- [8] L.V. Tsakanika, M.T. Ochsenkuhn-Petropoulou, L.N. Mendrinou, Investigation of the separation of scandium and rare earth elements from red mud by use of reversed-phase HPLC, *Anal. Bioanal. Chem.* 379 (5–6) (2004) 796–802.
- [9] K. Guclu, R.J. Apak, Modeling of copper (II), cadmium(II), and lead(II) adsorption on red mud from metal–EDTA mixture solutions, *J. Colloid Interface Sci.* 228 (2) (2000) 238–252.
- [10] P.E. Tsakiridis, S. Agatzini-Leonardou, P. Oustadakis, Tsakiridis red mud addition in the raw meal for the production of Portland cement clinker, *J. Hazard. Mater.* 116 (1–2) (2004) 103–110.
- [11] A. Akinci, H. Akbulut, F. Yilmaz, The effect of the red mud on polymer crystallization and the interaction between the polymer-filler, *Polym. Plast. Technol. Eng.* 46 (1) (2007) 31–36.
- [12] Strategic-Udy Metallurgical and Chemical Processes Limited (Hamilton, Canada), Process for the separation of iron, aluminium and titanium values from materials containing them, UK Patent GB843607, 1960.
- [13] A. Uzhidy, O. Borlai, P. Szabo, R. Jelinko, J. Szepvolgyi, G. Fenyi, M. Szabo, Processing low-quality alumina-containing ores by selective chlorination of iron, Hungarian Patent 181729, 1983.
- [14] E. Ercag, R. Apak, Furnace smelting and extractive metallurgy of red mud: recovery of TiO_2 , Al_2O_3 , and pig iron, *J. Chem. Technol. Biotechnol.* 70 (3) (1997) 241–246.
- [15] P. Kasliwal, P.S.T. Sai, Enrichment of titanium dioxide in red mud: a kinetic study, *Hydrometallurgy* 53 (1) (1999) 73–87.
- [16] S.S. Bhatnagar, S. Parthasarathy, G.C. Singh, A.L. Sundara Rao, Pilot plant for the recovery of titanium dioxide from bauxite sludge, *J. Sci. Ind. Res.* 4 (1945) 378–381.
- [17] E. Zimmer, A. Nafissi, G. Winkhaus, Reclamation treatment of red mud, US patent US4119698, 1978.
- [18] V. Damodaran, J. Gupta, Titanium dioxide from bauxite sludge, *J. Sci. Ind. Res.* 14B (1955) 292–297.
- [19] E. Sayan, M. Bayramoglu, Statistical modeling of sulfuric acid leaching of TiO_2 from red mud, *Hydrometallurgy* 57 (2) (2000) 181–186.
- [20] A. Atasoy, An investigation on characterization and thermal analysis of the Aughinish red mud, *J. Therm. Anal. Calorim.* 81 (2) (2005) 357–361.
- [21] G.E.P. Box, W.G. Hunter, J.S. Hunter, *Statistics for Experiments*, John Wiley, New York, 1978.